Available online at www.sciencedirect.com
ScienceDirect
Ceramics International 33 (2007) 1319–1324
CERAMICS INTERNATIONAL
www.elsevier.com/locate/ceramint

Addition of Al–Ti–B master alloys to improve the performances of alumina matrix ceramic materials

Changxia Liu [a,b,*], Jianhua Zhang [a,**], Junlong Sun [a,b], Xihua Zhang [c]

[a] Department of Mechanical Engineering, Shandong University, Jinan 250061, Shandong Province, PR China
[b] Communications Institute, Ludong University, Yantai 264025, Shandong Province, PR China
[c] Department of Materials Science and Engineering, Shandong University, Jinan 250061, Shandong Province, PR China

Received 13 January 2006; received in revised form 28 February 2006; accepted 11 April 2006
Available online 11 September 2006

Abstract

In the present work, a new technique to improve the performances of alumina matrix ceramic materials is presented, in which Al, Al_3Ti and TiB_2 are incorporated into alumina matrix ceramic materials in the form of Al–Ti–B master alloys. Composites of Al_2O_3/TiB_2/AlN/TiN are fabricated by the technology of transient liquid phase sintering, during which new phases such as AlN and TiN are produced by the chemical reactions taking place among Al, Ti and N_2 (the protective atmosphere). The densification rate of the composites as a function of Al–Ti–B volume content is discussed. The fundamental properties of the composites such as hardness, fracture toughness and bending strength are examined. The relations of volume content of Al–Ti–B master alloys and mechanical properties of alumina matrix ceramic materials are analyzed. The effects of fracture mechanism on mechanical properties of the composites are researched together with the refining performances of Al–Ti–B master alloys.

Keywords: B. Composites; Alumina; Al–Ti–B master alloys; Refining performances

1. Introduction

With several special properties like high hardness, good chemical inertness, high wear resistance and low cost, alumina is attracting considerable interest for advanced engineering applications such as refractory materials, grinding media, cutting tools, and high temperature bearings. However, the brittleness of monolithic Al_2O_3 limits its application in many engineering fields. It has been a key subject for many years that how to improve the bending strength and fracture toughness of monolithic Al_2O_3 [1–8]. Researchers have attempted to improve the mechanical properties of monolithic Al_2O_3 by incorporating intermetallic compounds such as Fe_3Al [9], Fe–Al [10] and AlTiC [11] into alumina matrix, and many interesting results have been obtained. The low price of Al–Ti–B master alloys permits its widespread applications to the refining technology of Al and its alloys [12,13], however, there are few articles reporting application of Al–Ti–B master alloys on refining alumina matrix ceramic materials.

Cai et al. [14] considered that AlN, which was formed by the reaction of Al and N_2 during the sintering process, could make significantly improvements in mechanical properties of Al_2O_3/TiC composites. As additives, TiN [15,16] and TiB_2 [17,18] also play important roles in toughening alumina matrix ceramic materials. Being composed of Al, Al_3Ti and TiB_2 phases [19], Al–Ti–B master alloys are introduced in alumina matrix ceramic materials with different volume contents, and N_2 is used as the protective atmosphere in the hot-pressing sintering process. The specific objective of the study is to determine whether Al in Al–Ti–B and Ti, being separated from Al_3Ti, can react with N_2 to produce AlN and TiN. Newly formed AlN and TiN phases can cooperate with TiB_2 to improve the performance of alumina matrix materials.

2. Experimental procedure

Commercial Al_2O_3 powder of high purity (99.99%) and small grain size (0.5–1 μm) was used as the starting materials. Al–Ti–B master alloys, which are developed by the department

* Corresponding author. Tel.: +86 531 82266727.
** Corresponding author.
E-mail addresses: hester5371@gmail.com (C. Liu), jhzhang@sdu.edu.cn (J. Zhang).

0272-8842/$32.00
doi:10.1016/j.ceramint.2006.04.014

Table 1
Compositions of hot pressed composites

Specimens	Composition
AT_0	100 vol.% Al_2O_3 + 0 vol.% Al–Ti–B
AT_5	95 vol.% Al_2O_3 + 5 vol.% Al–Ti–B
AT_{10}	90 vol.% Al_2O_3 + 10 vol.% Al–Ti–B
AT_{15}	85 vol.% Al_2O_3 + 15 vol.% Al–Ti–B
AT_{20}	80 vol.% Al_2O_3 + 20 vol.% Al–Ti–B
AT_{25}	75 vol.% Al_2O_3 + 25 vol.% Al–Ti–B

of materials science and engineering in Shandong University, were used as additives. The alloy used in present study has the composition Al–5% Ti–1% B. The volume content of Al–Ti–B master alloys ranged from 5 to 25 vol.% as listed in Table 1. (The suffix in AT_0, AT_5, AT_{10}, AT_{15}, AT_{20} and AT_{25} represents the volume content of Al–Ti–B. For example, AT_5 means the volume content of Al–Ti–B is 5 vol.%.)

The raw materials were blended with one other according to certain proportions and ball milled for 60 h in an alcohol medium to obtain a homogeneous mixture. Then the slurry was dried in vacuum and screened. Hot-pressing was used to sinter the powder mixture in a graphite die under nitrogen protection. The specimens were heated up to 1600 °C (30 °C min^{-1}) under a pressure of 30 MPa for 35 min.

The sintered specimens were machined with a grinding machine. Standard test pieces (3 mm × 4 mm × 36 mm) were obtained through rough grinding, finish grinding with diamond wheels, and polishing. Three-point-bending mode was used to measure the bending strength with a span of 20 mm and at a crosshead speed of 0.5 mm/min. The bending strength was calculated by the following formula [20]:

$$\sigma_f = \frac{3PL}{2bh^2} \quad (1)$$

where σ_f is bending strength (MPa) and P is load (N) under which the samples break, b and h are width and height (mm), respectively, and L is span (mm).

Vickers hardness was measured on polished surface with a load of 9.8 N for 5 s with a micro-hardness tester (MH-6). Fracture toughness measurement was performed using indentation method with a hardness tester (Hv-120), and results were obtained by the formula proposed by Cook and Lawn [21].

The X-ray diffraction (XRD) analysis was undertaken to identify the crystal phases present before and after sintering. Microstructural observations of fracture surfaces were done by scanning electron microscopy (HITACHI S-570).

3. Results and discussion

3.1. X-ray diffraction phase analysis

The X-ray diffraction analysis of AT_{15} powders before sintering and AT_{15} specimen after sintering at 1600 °C, under 30 MPa for 35 min, are shown in Figs. 1 and 2, respectively. It is clear from Fig. 1 that there exist Al_2O_3, TiB_2, Al_3Ti and Al phases in the ball-milled powders, which indicates that Al–Ti–B master alloys are composed of TiB_2, Al_3Ti and Al phases [19]. Further, there exist in AT_{15} specimen the Al_2O_3, TiB_2, TiN and AlN phases. Newly formed TiN and AlN may be produced in the following ways: when the temperature goes up to 1000 °C [22], labile Al_3Ti will dissolve to deliver Ti and Al particles:

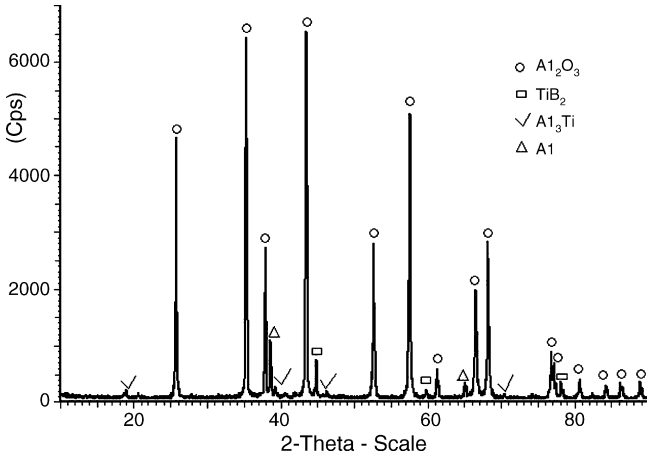

Fig. 1. XRD pattern of AT_{15} powder before sintering

$$Al_3Ti \rightarrow 3Al + Ti \quad (2)$$

The sintering temperature is 1600 °C, which is higher than the melting point of Al (660 °C). Hence, previously mentioned Al in Al–Ti–B master alloys and the delivered Al may be in the molten state, some may escape during the sintering process, the other reacting with N_2 (the protective atmosphere) to form the new phase AlN:

$$2Al + N_2 \rightarrow 2AlN \quad (3)$$

TiN is from the reaction taking place between delivered Ti and N_2:

$$2Ti + N_2 \rightarrow 2TiN \quad (4)$$

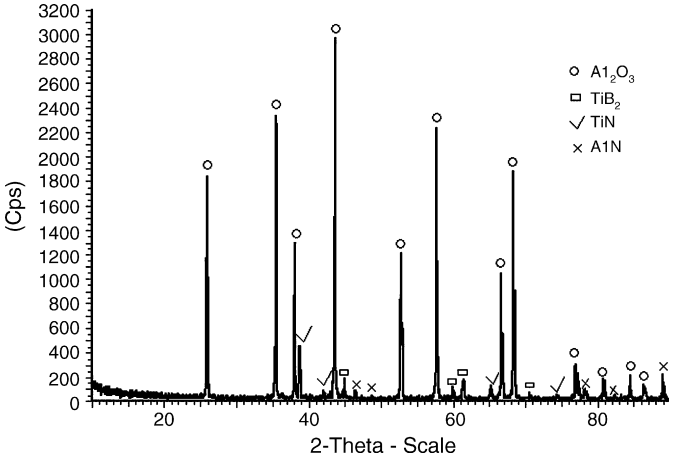

Fig. 2. XRD pattern of AT_{15} specimen after sintering.

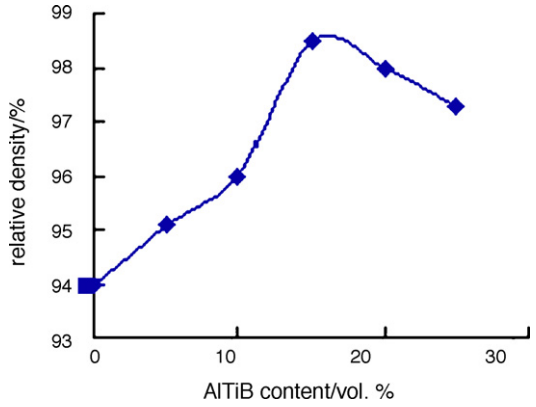

Fig. 3. Relation of Al–Ti–B content and relative density.

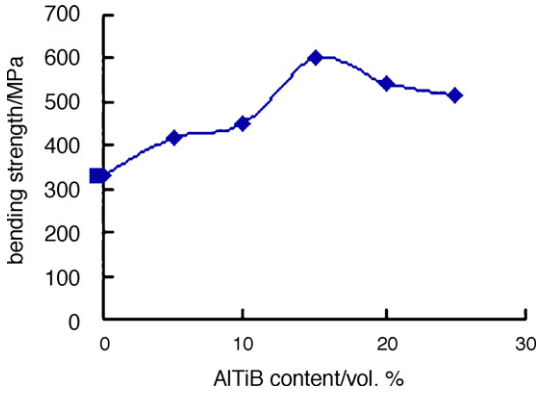

Fig. 5. Relation of Al–Ti–B content and bending strength.

Based on thermodynamic analysis of the reactions, we can get the following rankings [23]:

$$\Delta G^{\theta}_{T2\,(1273\,\mathrm{K})} = -182549.9635 < 0, \qquad \Delta G^{\theta}_{T3\,(1873\,\mathrm{K})} = -218483.1739 < 0, \qquad \Delta G^{\theta}_{T4\,(1873\,\mathrm{K})} = -324689.4844 < 0$$

where $\Delta G^{\theta}_{T2\,(1273\,\mathrm{K})}$, $\Delta G^{\theta}_{T3\,(1873\,\mathrm{K})}$ and $\Delta G^{\theta}_{T4\,(1873\,\mathrm{K})}$ represent the Gibbs free energy of the reactions (2)–(4), respectively, and the temperature are 1000, 1600, and 1600 °C, respectively. The XRD analysis shows that Al_2O_3, TiB_2, TiN and AlN phases actually exist in sintered specimen of AT_{15} as previously mentioned.

3.2. Densification of the composites

Fig. 3 shows the relative density curves for AT_0, AT_5, AT_{10}, AT_{15}, AT_{20} and AT_{25} sintered at 1600 °C, under 30 MPa for 35 min. It is clear from the figure that the relative density of AT_0 is only 94%, and that of the $Al_2O_3/TiB_2/AlN/TiN$ composites increases sharply (up to 98.5%) as the addition amount of Al–Ti–B master alloys is raised from 0 to 15 vol.%. This trend reverses with further addition of Al–Ti–B master alloys, and the relative density of AT_{25} specimen decreases to 97.3%. This is mainly because the amount of TiB_2, which is difficult to be densified [24], is increasing. Obviously, the densification rate of the composites increases with the volume content of Al–Ti–B master alloys increasing from 0 to 15%. The highest relative density value of AT_{15} is enhanced by 4.8% compared to that of monolithic Al_2O_3.

3.3. Mechanical properties

The relations of Al–Ti–B volume content and hardness, bending strength, fracture toughness of hot-pressed alumina matrix ceramic materials are shown in Figs. 4–6, respectively. The hardness and bending strength of monolithic Al_2O_3 is respectively 17.64 GPa and 331.5 MPa, and the fracture toughness is 3.52 MPa $m^{1/2}$. Kim et al. [25] have observed that the mechanical properties such as hardness, fracture toughness and strength of the composites increase as the improvements in the relative density of sintered specimens are obtained. As seen from Figs. 4–6, the variation in hardness, fracture toughness and strength of the composites with Al–Ti–B volume content is analogous to that of relative density curve. The hardness of the composites increases as Al–Ti–B content is raised from 0 to 10 vol.% and reaches its maximum value of 21 GPa, then decreases from 10 to 25 vol.%. As a general rule, the hardness of the composites should decrease with the increasing amount of low-hardness Al–Ti–B, whereas the curve in Fig. 4 is a parabola with a maximum value. There are two factors influencing the hardness of composites, namely a

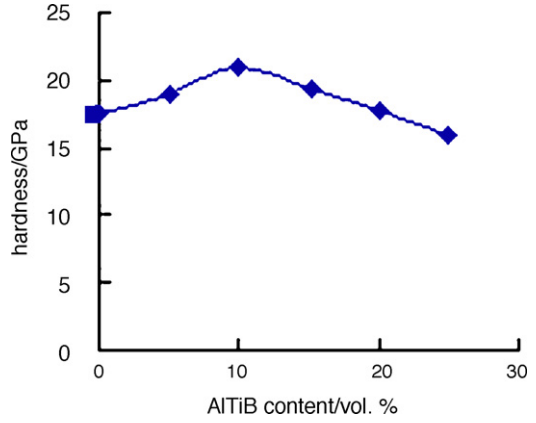

Fig. 4. Relation of Al–Ti–B content and hardness.

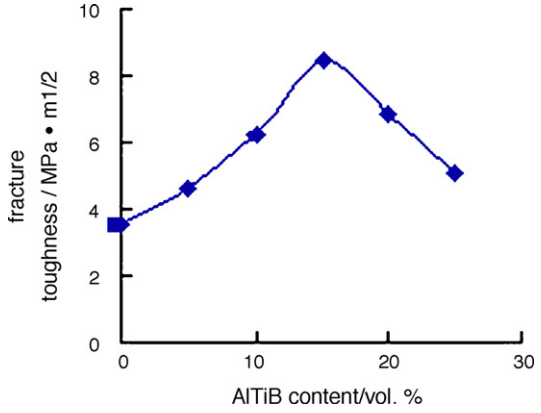

Fig. 6. Relation of Al–Ti–B content and fracture toughness.

hardness effect due to the addition of Al–Ti–B master alloys and a densification effect of the composites. The hardness of the composites increases for the reason that the densification effect is stronger than the hardness effect, otherwise the hardness of the composites will decrease. In the first stage (0 to 10 vol.% addition), the densification effect is dominant and the hardness is enhanced, while the hardness is reduced as the hardness effect is in turn becoming dominant (10–25 vol.% addition). The effects of Al–Ti–B master alloys on the bending strength and fracture toughness of the composites are similar to each other as shown in Figs. 5 and 6. They increase with the increasing amount of Al–Ti–B master alloys before 15 vol.%, and then reach their maximum values. For 15 vol.%, the bending strength and toughness are 600 MPa, 8.44 MPa $m^{1/2}$, respectively, and decrease after 15 vol.%. This trend of bending strength and fracture toughness correlates with the microstructures of the composites, which will be discussed in the following section.

It is obvious that the fabricated $Al_2O_3/TiB_2/AlN/TiN$ composites, sintered at 1600 °C, under 30 MPa for 35 min, exhibit significant improvements in mechanical properties than monolithic Al_2O_3. Composite with the addition of 15 vol.% Al–Ti–B master alloys shows better comprehensive performances, the hardness, bending strength and the fracture toughness of the composite reach 19.3 GPa, 600 MPa and 8.44 MPa $m^{1/2}$, respectively, which are enhanced by 9.41, 81 and 139.8%, respectively, with respect to monolithic Al_2O_3 sintered under the same conditions.

3.4. Analysis of microstructures

SEM photomicrograph of fracture surface of monolithic Al_2O_3 sintered at 1600 °C is shown in Fig. 7, those of AT_5, AT_{15} and AT_{25} are shown in Figs. 8–10, respectively. There are

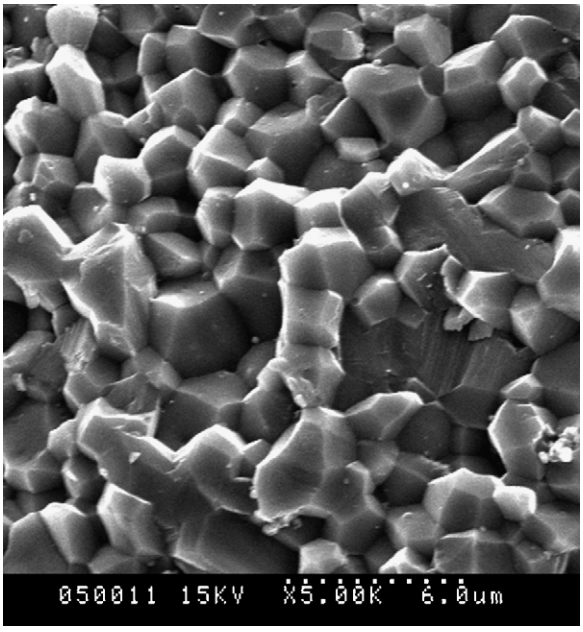

Fig. 8. SEM photomicrograph of AT_5 specimen.

significant microstructural differences among the composites. The fracture mode of monolithic Al_2O_3 is mainly intergranular failure, and the mean grains size is about 20 μm. The addition of Al–Ti–B master alloys makes the microstructures of the composites finer and more homogeneous. The fracture mode keeps invariant with incorporation of 5 vol.% Al–Ti–B master alloys and then turns to the combination of transgranular failure and intergranular failure as the addition amount of Al–Ti–B master alloys reaches 15 vol.%, as is shown in Figs. 8 and 9. Further addition of Al–Ti–B master alloys (25 vol.%) makes the fracture mode mainly intergranular failure, which is accompanied with little transgranular failure (Fig. 10). It can be

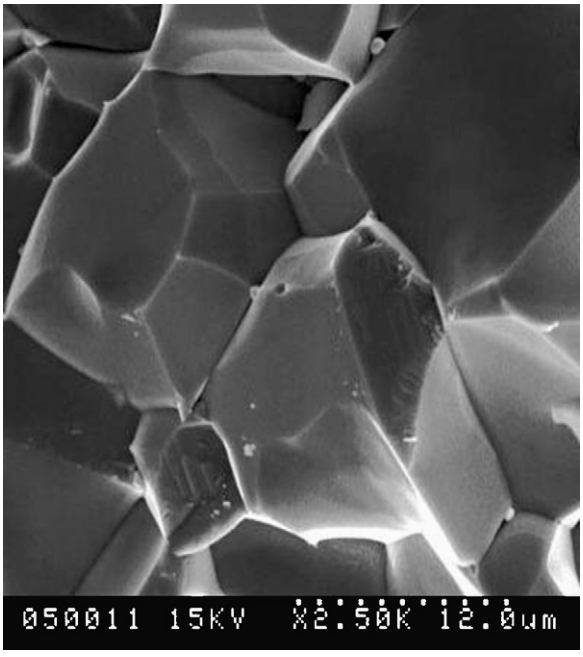

Fig. 7. SEM photomicrograph of monolithic Al_2O_3.

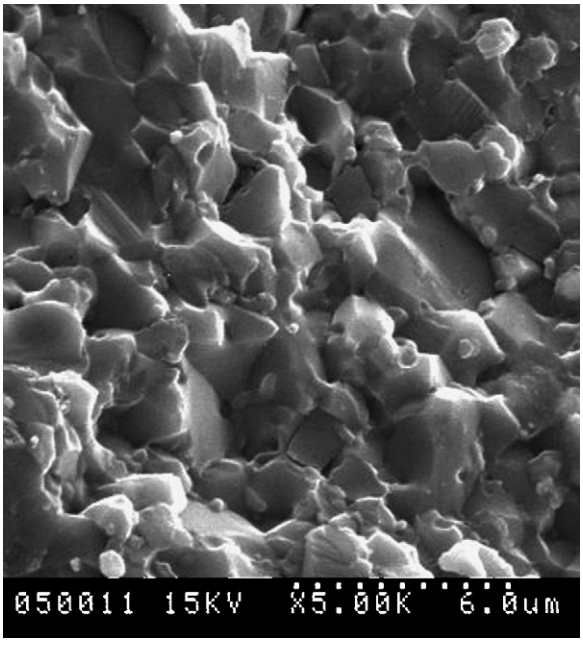

Fig. 9. SEM photomicrograph of AT_{15} specimen.

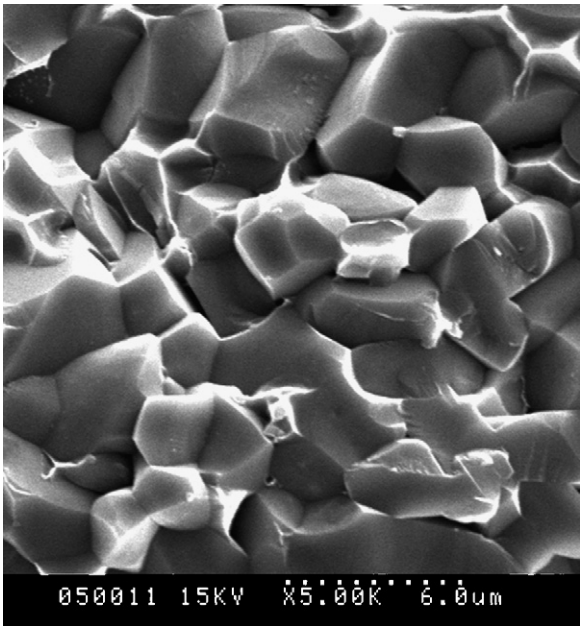

Fig. 10. SEM photomicrograph of AT_{25} specimen.

seen from Fig. 9, the bondings of grains become stronger when the fracture mode turns to the combination of transgranular failure and intergranular failure. In other words, a fracture mode changing from intergranular failure to the combination of transgranular failure and intergranular failure is observed and may bring on a significant increase in bending strength and fracture toughness. The main cause is that the grain boundaries of the composites are strengthened owing to the addition of Al–Ti–B master alloys.

The mean grains size of monolithic Al_2O_3 is about 20 μm as previous mentioned, while that of AT_5, AT_{15} and AT_{25} are 3, 2 and 5 μm, respectively. The grains size of monolithic Al_2O_3 is larger than that of the composites toughened by Al–Ti–B master alloys under identical conditions. It indicates that the grains of Al_2O_3 in composites may be restrained from abnormal growth owing to the addition of Al–Ti–B master alloys. The reason is as follows, Al–Ti–B master alloys are composed of TiB_2, Al_3Ti and Al phases, the melting point of Al is 660 °C, so the liquid-phase sintering begins as the temperature goes above 700 °C. The reaction between Al and N_2 first occurs on the surface of the disc compacts. However, this development of the reaction is slow owing to high chemical bond strength of Nitrogen molecule and it is difficult for N_2 to infiltrate through the compacted AlN by reason of the very low solubility of N_2 in Al and strong compactness of AlN. So it takes long time to complete the transformation of Al to AlN [14]. $TiAl_3$ can be a very effective nucleant for aluminum [13], but this phase dissolves quickly under the sintering temperature and then Ti is provided by the dissolution of $TiAl_3$. It has been reported that Ti plays a significant role in refining pure Al [26]. Furthermore, TiB_2 particles are dispersed and being virtually insoluble in molten aluminum, act as heterogeneous nucleation sites. The behavior is merely a result of particle setting and agglomeration [12]. The existing of Ti changes the interface between liquid Al and solid alumina, and its reaction with N_2 or O (O is provided by alumina, the compounds of Ti and O are too small to be detected by XRD analysis.) improves the wettability of Al and alumina [27,28]. When the temperature is 800–1000 °C, dissolution of alumina in Al occurs, and upon cooling alumina crystals heteroepitaxially nucleate on the pre-existing alumina grains, leading to grain refinement. At the end of the sintering process, expect those may have escaped by the way of flowing out or vaporizing, Al is almost entirely transformed into AlN, which has a grains size on the order of nanometers. These nanometer grains of AlN and TiN, which are formed by in situ synthesis, distribute evenly over alumina matrix ceramic materials and contribute to the refining effect [14].

4. Conclusion

$Al_2O_3/TiB_2/AlN/TiN$ composites are fabricated by hot-pressing technology. Transient liquid phase sintering comes into being, during which new phases such as AlN and TiN are produced by the chemical reactions taking place among Al, Ti and N_2. The relative density of AT_{15} specimen reaches its maximum value of 98.5%. The composite with the addition of 15 vol.% Al–Ti–B master alloys shows better comprehensive performances, and the hardness, bending strength and the fracture toughness of the composite are 19.3 GPa, 600 MPa and 8.44 MPa $m^{1/2}$, respectively. The fracture mode of monolithic Al_2O_3 is mainly intergranular failure. The addition of Al–Ti–B master alloys makes the microstructures of the composites finer and more homogeneous. The fracture mode turns to the combination of transgranular failure and intergranular failure as the addition amount of Al–Ti–B master alloys is 15 vol.%, which may bring on the increase in bending strength and fracture toughness. One of the main causes is that the grain boundaries of the composites are strengthened, and the other is that the grains of Al_2O_3 in composites may be restrained from abnormal growing owing to the addition of Al–Ti–B master alloys.

Acknowledgements

The work described in this paper is supported by the Ministry of Education, P.R. of China (No. 03101) and the Outstanding Young Scientist Rewards of Shandong Province (No. 03BS103).

References

[1] Y. Ji, J.A. Yeomans, Processing and mechanical properties of Al_2O_3–5 vol.% Cr nanocomposites, J. Eur. Ceram. Soc. 22 (2002) 1927–1936.
[2] S.K.C. Pillai, B. Baron, M.J. Pomeroy, S. Hampshire, Effect of oxide dopants on densification, microstructure and mechanical properties of alumina–silicon carbide nanocomposite ceramics prepared by pressureless sintering, J. Eur. Ceram. Soc. 24 (2004) 3317–3326.
[3] D.H. Riu, Y.M. Kong, H.E. Kim, Effect of Cr_2O_3 addition on microstructural evolution and mechanical properties of Al_2O_3, J. Eur. Ceram. Soc. 20 (2000) 1475–1481.
[4] L. Wang, J.L. Shi, Z.L. Hua, J.H. Gao, D.S. Yan, The influence of addition of WC particles on mechanical properties of alumina–matrix composite, Mater. Lett. 50 (2001) 179–182.

[5] Y.Q. Fu, Y.W. Gu, H.J. Du, SiC whisker toughened Al_2O_3–(Ti, W) C ceramic matrix composites, Scr. Mater. 44 (2001) 111–116.
[6] S. Postrach, J. Potschke, Pressureless sintering of Al_2O_3 containing up to 20 vol.% zirconium diboride (ZrB_2), J. Eur. Ceram. Soc. 20 (2000) 1459–1468.
[7] V.M. Sglavo, F. Marino, B.R. Zhang, S. Gialanella, Ni_3Al intermetallic compound as second phase in Al_2O_3 ceramic composites, Mater. Sci. Eng. A 239–240 (1997) 665–671.
[8] R.G. Wang, W. Pan, J. Chen, M.H. Fang, M.N. Jiang, Z.Z. Cao, Microstructure and mechanical properties of machinable $Al_2O_3/LaPO_4$ composites by hot pressing, Ceram. Int. 29 (2003) 83–89.
[9] Y.S. Yin, H.Y. Gong, J. Li, Preparation and properties of Al_2O_3/Fe_3Al composite, J. Chin. Ceram. Soc. 31 (8) (2003) 721–726 (in Chinese).
[10] Y.J. Zhang, Y.S. Yin, Z.C. Bao, Study on Fe–Al intermetallic compounds/Al_2O_3 ceramic composites, Bull. Chin. Ceram. Soc. 19 (4) (2000) 39–42 (in Chinese).
[11] X.H. Zhang, C.X. Liu, J.H. Zhang, Preparation of alumina matrix ceramic composite materials by hot-press sintering process, J. Chin. Ceram. Soc. 33 (7) (2005) 14–18 (in Chinese).
[12] C. Limmaneevichitr, W. Eidhed, Fading mechanism of grain refinement of aluminum–silicon alloy with Al–Ti–B grain refiners, Mater. Sci. Eng. A 349 (2003) 197–206.
[13] A.L. Greer, A.M. Bunn, A. Tronche, P.V. Evans, D.J. Bristow, Modelling of inoculation of metallic melts application to grain refinement of aluminium by Al–Ti–B, Acta Mater. 48 (2000) 2823–2835.
[14] K.F. Cai, C.W. Nan, R.Z. Yuan, Preparation and microstructure analysis of Al_2O_3–AlN–TiC composite ceramic, J. Chin. Ceram. Soc. 23 (4) (1995) 430–433 (in Chinese).
[15] Z.S. Rak, J. Czechowski, Manufacture and properties of Al_2O_3–TiN particulate composites, J. Eur. Ceram. Soc. 18 (4) (1998) 373–380.
[16] E. Laarz, M. Carlsson, B. Vivien, M. Johnsson, M. Nygren, L. Bergström, Colloidal processing of Al_2O_3-based composites reinforced with TiN and TiC particulates, whiskers and nanoparticles, J. Eur. Ceram. Soc. 21 (8) (2001) 1027–1035.
[17] J.X. Deng, T.K. Cao, L.L. Liu, Self-lubricating behaviors of Al_2O_3/TiB_2 ceramic tools in dry high-speed machining of hardened steel, J. Eur. Ceram. Soc. 25 (7) (2005) 1073–1079.
[18] J.X. Deng, X. Ai, J.S. Zhang, Effect of whisker orientation on the friction and wear behaviour of $Al_2O_3/TiB_2/SiC_\omega$ composites in sliding wear tests and in machining processes, Wear 201 (1–2) (1996) 178–185.
[19] K.B. Yin, X.F. Bian, Y. Zhao, J.K. Zhou, N. Han, Grain refining performances of Al–5Ti–1B master alloy for cast Al–10Mg alloy, Foundry 54 (2) (2005) 138–140.
[20] Z.H. Jin, J.Q. Gao, G.H. Qiao, Eng. Ceram. [M], Publishing House of Xian Jiao Tong University, Xian, 2000 (in Chinese).
[21] R.F. Cook, B.R. Lawn, A modified indentation toughness technique, J. Am. Ceram. Soc. 66 (11) (1983) 200–201.
[22] X.F. Liu, X.F. Bian, Y. Yang, et al., The formation law of $TiAl_3$ morphologies in AlTi5B master alloy, Special Casting Nonferr. Alloys 5 (1997) 4–6 (in Chinese).
[23] D.L. Ye, J.H. Hu, Handbook of the Thermodynamic Data of Inorganic Substances, Metallurgical Industry Press, Peking of China, 2002, pp. 57–1061.
[24] M.A. Meyers, E.A. Olevsky, J. Ma, M. Jamet, Combustion synthesis/densification of an Al_2O_3–TiB_2 composite, Mater. Sci. Eng. A 311 (1–2) (2001) 83–99.
[25] H.W. Kim, Y.H. Koh, H.E. Kim, Densification and mechanical properties of B_4C with Al_2O_3 as a sintering aid, J. Am. Ceram. Soc. 83 (11) (2000) 2863–2865.
[26] Z.Q. Wang, X.F. Liu, X.F. Bian, Phases and refinement performances of AlTiC master alloys[J], Foundry 50 (6) (2001) 316–320 (in Chinese).
[27] C.G. Wan, P. Kritsalis, N. Eustathopulos, Wettability and interfacial metallurgical behaviour of high temperature brazing alloys (PdCu–Ti) on alumina[J], Transact. China Weld. Inst. 15 (4) (1994) 209–213 (in Chinese).
[28] G.Y. Li, H. Nakae, T. Hane, et al., The improvement of wettability of Al_2O_3 by molten aluminum[J], J. Mater. Eng. 4 (2000) 11–13 (in Chinese).